MAPPING COMPLEX SOIL-LANDSCAPE PATTERNS USING RADIOMETRIC K%: A DRY SALINE LAND FARMING AREA CASE STUDY NEAR JAMESTOWN, SA

Mark Thomas[1], Rob W. Fitzpatrick[2] and Graham S. Heinson[3]

[1] CRC-LEME/University of Adelaide, PMB 2, Glen Osmond, Adelaide, SA 5064
[2] CRC-LEME/CSIRO Land and Water, PMB 2, Glen Osmond, Adelaide, SA 5064
[3] CRC-LEME/University of Adelaide, North Terrace, Adelaide, SA 5000

INTRODUCTION

Location

The study area ("Cootes' site") straddles two farms in South Australia's NAD, and covers an area of 121 ha. To the north is Jamestown (25 km), and to the south Spalding (20 km) and Adelaide (180 km) (Figure 1a). The study site is on the east flank of a broad north-south valley system (Figure 1b), drained southwards by the "Freshwater Creek". The site is on the east flank of the valley. The crest-to-valley bottom toposequence (A/B) (inset, Figure 1b) length is 1,500 m, and has a relief difference of 100 m, i.e., 470-370 m. A basement of tillites, quartzites, mudstones, siltstones and shales underlies the toposequence. A prominent feature of the landscape is the deeply incised (12 m) erosional gully formed by the creek. 75% of the 450 mm annual rainfall falls in the winter growing season (May to October).
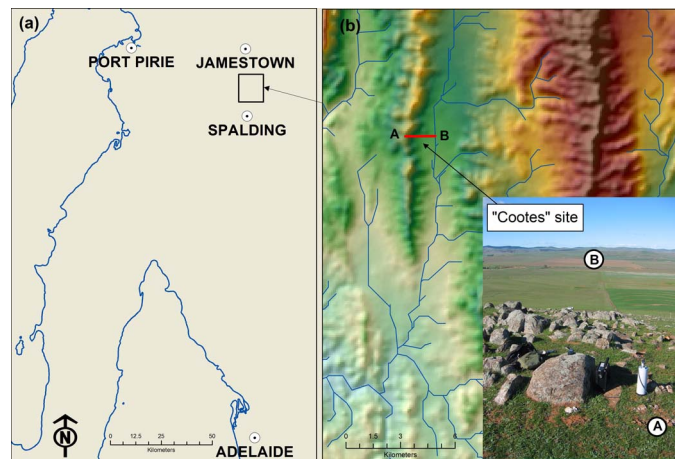

Figure 1: Study area regional context (a), and landscape location with toposequence A/B marked (b). Inset, photo of study area looking from A to B.

Dry saline land forming factors

Dry saline land occurs in the upper parts of the landscape not influenced by deep saline groundwater (Fitzpatrick *et al.* 2003a, b). This landscape context is totally unlike that of "dryland salinity", which occurs in low parts of landscapes where saline groundwater tables are close to or at the surface. Dry saline land is found in upland, winter-rainfall zones in South Australia that are usually semi-arid. Typical salinities on the soil surface range from EC_{se} 4-60 dS/m (surface form) and EC_{se} 2-8 dS/m in the subsoil (i.e., 0.3-1.0 m) (subsoil form), and present a hazard to agriculture in increasing concentrations.

The development of dry saline land salinity is strongly associated with texture-contrast (duplex) soils (e.g., loams over clays) in which key soil-landscape processes include sodification and salinisation. On wetting, sodicity causes general subsoil structural decline as clay aggregates disintegrate, disperse and clog soil pores. Sodic pore clogging in the A-B horizon interface creates a layer that is almost impermeable to vertical water movement. Consequently, during winter when up-slope soils are wettest, subsoil water movement is lateral (i.e., down slope), through the courser-textured A horizon. Locally, this results in the formation of wet patches (i.e., perched watertables) in depressions, break-of-slopes, and where upper layer soil textures become clayier down-slope at soil unit transitions. However, where subsoil freshwater flow rates are high enough, i.e., in drainage zones on steep slopes, subsoil salts are washed out. Over time the perched watertables accumulate salts. Subsequently, during warm dry summer periods, the combination of surface

evaporation and subsoil evapotranspiration creates dynamic moisture conditions in the subsoil profile. These conditions cause dissolved salts to mobilise through the subsoil profile with the wetting front, and to concentrate in topsoil and subsoil layers as they dry (Rengasamy 2002). The seasonally changing salt concentrations in these layers—both temporally and spatially—pose a considerable farming challenge, often compounded by the associated problems of waterlogging and/or sodic structural decline in the soil.

DATA SETS AND INTERPRETATION

Soil and landscape data
The interpretation of dry saline land soil-landscape processes in the study area is described in Fitzpatrick *et al.* (2003a). This work relied on previous soil mapping and laboratory analysis (Fitzpatrick *et al.* 2003c), geology, a digital elevation model, and volume magnetic susceptibility and electromagnetic (EM) data from labour-intensive ground surveys.

The study area was divided into a number of landscape soil units (LSUs) based on similarities in: morphology (soil texture, layers, structure, etc.); zones of salt accumulation; and hydrology (i.e., groundwater and freshwater flows). These, with the laboratory analysis data (clay %, EC_{se} and ESP), are shown in Figure 2, over laid on a 3-D aerial photo drape. Also shown are the locations of soils ("a" and "b" from < 0.3 m, and "c" at 1.0 m) and taken for XRD analysis.

Briefly, LSU 1-type soils are shallow loams on the crest, interspersed with outcropping (i.e., 5-50% surface cover) shales and siltstones. LSU 2-type soils are saline/sodic clays on steep upper slopes. LSU 3-type soils are on lower colluvial/alluvial slopes, and demonstrate strong texture contrasts between the leached upper layer loams above sodic clay layers (refer to Figure 2 profile data). LSU 4-type soils are deep alluvial sodic clays with thin leached A horizons.

EM surveys
The EM surveys were conducted using an EM38 (Figure 3a) and an EM31 (Figure 3b) (Fitzpatrick *et al.* 2003a). The EM38 determines subsoil conductivity at approximately 0.75 m deep, and the EM31, the regolith conductivity at approximately 6 m deep. Figure 3 shows high conductivity values in red, medium values in yellow-turquoise, and low values in dark blue. Conductivity values are generally strongly related to salt content (apparent EC).

Salt distribution
Figure 3a (EM38) displays three zones of relatively high subsoil conductivity. Feature "m" in LSU 2 is likely to represent an area of near-surface mineralisation. LSU 3 displays regions of conductivity associated with sloping areas that are not in drainage zones. These regions are likely to represent subsoil salts, and are indicative of the subsoil form of dry saline land discussed earlier. Moderate conductivities are displayed throughout LSU 4 areas, and are likely to be associated with low salt concentrations in the subsoil (ref. Figure 2 profile data).

By contrast, the EM31 plot (Figure 3b) shows regolith (6 m) conductivity in all LSUs, especially in the drainage zones on sloping areas, and throughout LSU 4. A large proportion of high conductivity response on the sloping areas is probably associated with conductive basement rock or the deposition of magnetic colluvial material. In the sloping area drainage zones the highly conductive regolith pattern is likely to reflect magnetic colluvial material and/or salt accumulation. These salts are likely to have been washed down from upper-slope areas, or from below in saline groundwater. The LSU 3/4 boundary forms a prominent contrasting conductivity feature. The high conductivity throughout most of LSU 4 is likely to reflect the hydraulic barrier - caused by the low sodic clay permeability - which traps and concentrates up-slope regolith salts. Perhaps after a considerable time in storage the salts seep out of the gully face, evidenced by high EM31 conductivity zones and laboratory data.

The conductivity patterns from Figure 3, combined with soil profile data (ESP, salinity and clay %) in A and B horizons in Figure 2, suggest that soil-landscape patterns with LSU 3-type soils up-slope of LSU 4-type soil are likely to be indicative of landscapes prone to dry saline land formation and salt entrapment - along with the attendant soil issues discussed earlier. Therefore, this type of soil-landscape pattern expressed in areas with similar environmental conditions (e.g., climate, geology, land use) is likely to be a useful predictor of where these soil issues are likely to occur in the landscape. If so, the ability to predict these patterns will be important in managing these areas more effectively.
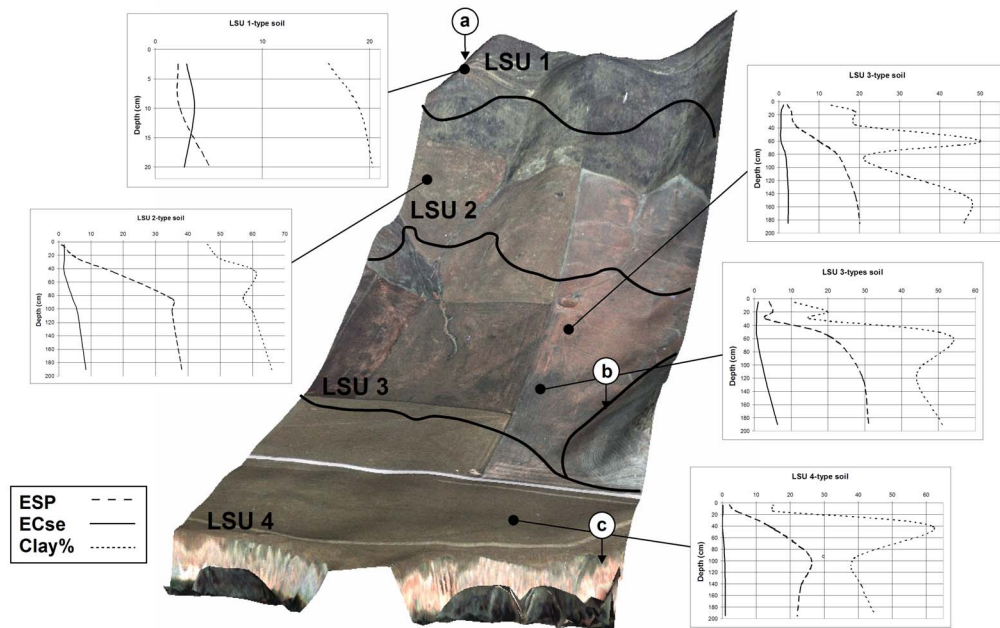
Figure 2: 3-D aerial photo drape of the study area with landscape soil unit boundaries, laboratory data and XRD sampling locations indicated.
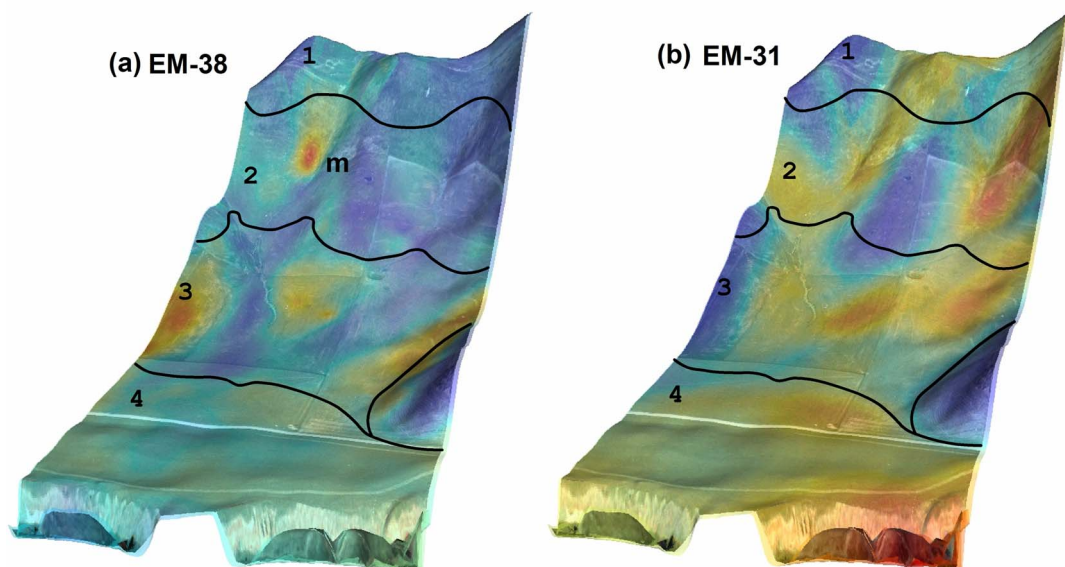

Figure 3: EM38 (a) and EM31 (b) surveys over laid on a 3-D aerial photo drape of the study area. High conductivity values are in red, medium values in yellow-turquoise, and low values in dark blue.

Airborne K% radiometrics

Airborne radiometrics measure the gamma activity released in the radio-decay of K, Th and U in the top 0.35 m of the land surface (Minty 1997). Depending on the specific survey requirements and data application, acquisition costs can be cost-effective, e.g., A$1.80 per ha or less. The farm scale (i.e., 20 m resolution) airborne radiometrics used in the study was acquired through NAP as part of South Australian Salt Mapping and Management Support Project (Munday *et al.* 2003).

The airborne K% distribution in the study area is shown in Figure 4. The values range from 1.1% to 2.5%. High K% values are shown in red and low values in yellow. Figure 4 shows a strong pattern of high K% values in the LSU 4-type soils, and generally lower values throughout the rest of the landscape soil units in the study area. The LSU 3/4 boundary forms a prominent contrasting K% feature, very similar to the strong contrast seen in the EM31 regolith conductivity (Figure 3b) in the same part of the landscape.
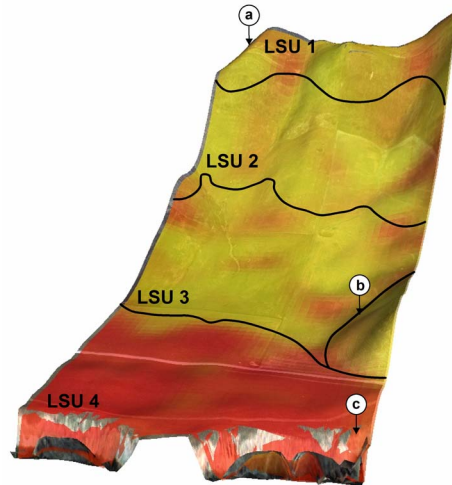
Figure 4: Study area airborne radiometric K% distribution over laid on a 3-D aerial photo drape. High K% values are in red, low values in yellow. XRD sampling locations (a, b and c) are indicated.

Airborne radiometric K% validation

A regression analysis was conducted to determine airborne K% accuracy. This involved conducting 53 field K% readings using a hand held gamma-ray radiometer (taken over 250 seconds for a sufficient count rate) throughout the study area (Figure 5).

These readings were co-registered to the airborne K% using a geographic information system, and a regression analysis conducted on the paired data. Figure 6 shows a reasonably strong R^2 value of 0.75, initially indicating a useful relationship between airborne and field K%. An important contributor to the variation seen in the two data sets is due to the large ground footprint acquired by the airborne sensor (i.e., mixing the signal from all surface materials in the footprint, e.g., soils, rocks, etc.) compared to the comparatively very small area of soil signal acquired in the field using the hand held radiometer.
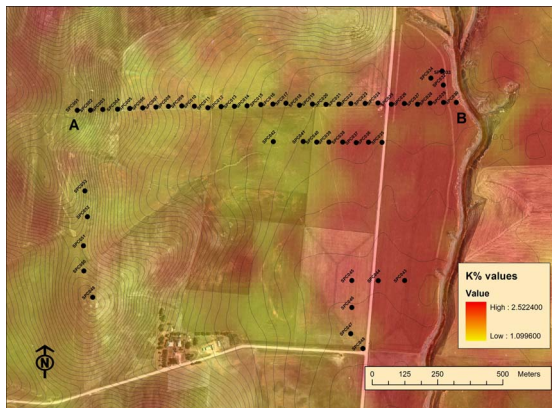

Figure 6: Locations of field hand held gamma-ray spectrometer readings, over laying 2 m contours, airborne K% coverage and aerial photo of the study area.
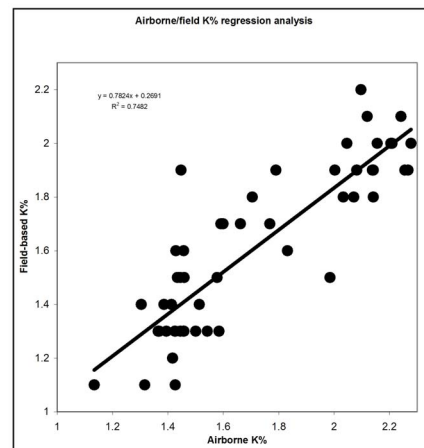

Figure 5: Airborne (X-axis) versus field based (Y-axis) K% radiometric regression plot.

Clay mineralogy

Preliminary XRD analysis on the clay fractions from soil samples "a", "b" and "c" (Figures 2 and 4) was conducted. The results are shown in Table 1, with airborne K% and soil clay %.

This investigation indicates that chlorite dominates the < 0.25 m depth clay fraction of the crest (LSU 1) and the < 0.35 m depth clay fraction of the sloping area (LSU 3) soils, while mica and smectite co-dominate the clay fraction at 1.0 m in the LSU 4-type soil.

Table 1. XRD interpretation for soil samples "a", "b" and "c" with airborne K% and soil clay %.

Site	Depth range (m)	XRD interpretation	Airborne K%	Ave. soil clay content (%)
a	0.0-0.25	Chlorite dominant	1.8	18
b	0.0-0.35	Chlorite dominant	1.5	21
c	1.0	Mica and smectite co-dominant	2.1	35

LINKING CLAY MINERALOGY, DRY SALINE LAND PROCESS AND AIRBORNE RADIOMETRICS

Mica, smectite and chlorite are soil-clay fraction layer silicates. Both mica and smectite have a high K content, while chlorite has a low K content (Taylor and Eggleton 2001). By combining the results of the XRD analysis, soils data, and airborne K% distribution, the following study area patterns are revealed: mica and smectite dominate areas that spatially coincide with (i) high airborne K% areas and (ii) LSU 4-type soils. Chlorite dominated areas spatially coincide with (i) low airborne K% areas, and (ii) LSU 1, 2 and 3-type soils. Soil data from Figure 2 indicates that low airborne K%/LSU 1, 2 and 3 areas have subsoil dry saline land salinity due to maximum salinity values at <1 m depth ranging between EC_{se} 2.5-5.5 dS/m. However, high airborne K%/LSU 4-type soils do not demonstrate dry saline land conditions. The reduced hydraulic permeability in the subsoil of the LSU 4-type soils from the sodic mica/smectite clay dispersion is likely to create the hydraulic conditions for dry saline land formation in the up-slope, LSU 3-type soils, i.e. impeded subsoil freshwater flow, perched watertable formation, and finally subsoil salt accumulation. Therefore, patterns showing low airborne K% areas (LSU 3-type soils) up-slope of high airborne K% areas (LSU 4-type soils) may provide the spatial "clues" for the prediction of dry saline land-prone landscapes in up-slope, LSU 3-type soils.

CONCLUSIONS

This study in an area characterised by a complex mosaic of soils with dry saline land conditions - along with attendant waterlogging, sodicity and fertility issues - has enabled us to establish relationships between (i) landscape soil units, and subsoil and regolith salt distributions from ground-based EM, terrain, soil survey and laboratory analysis data; (ii) landscape soil units and upper layer clay mineralogy; and (iii) clay mineralogy and airborne K% radiometrics. Based on the discussion in previous sections on soil-landscape arrangements being likely precursors to dry saline land conditions, the patterns derived from cost-effective airborne K% imagery are likely to be helpful in the pursuit of an airborne methodology to predict dry saline land soil patterns in landscapes under similar environmental conditions for farming purposes. A regression relationship of R^2 0.75 between airborne and ground based K% initially indicates confidence in the accuracy of the airborne K%.

Future work will focus on quantitative XRD analysis to confirm airborne radiometrics K, Th and U/clay mineral and heavy metal relationships in the landscape from samples acquired during the validation fieldwork (Figure 5). We will also develop a stronger understanding of soil-landscape patterns employing, for example, subsoil B horizon micro-relief analysis, surface terrain analysis, and airborne magnetic imagery acquired through NAP.

REFERENCES

FITZPATRICK R.W., DAVIES P.J., THOMAS M. & WILLIAMS B. 2003a. *Dry saline land: an investigation using ground-based geophysics, soil survey and spatial methods near Jamestown, South Australia.* CSIRO Land and Water, Adelaide.

FITZPATRICK R.W., MERRY R.H., COX J., RENGASAMY P. & DAVIES P.J. 2003b. *Assessment of physico-chemical changes in dryland saline soils when drained or disturbed for developing management options.* CSIRO Land and Water, Adelaide, pp. 57.

FITZPATRICK R.W., THOMAS M., CANNON M.G., MCTHOMPSON J. & COOTES T.R. 2003c. *Soils and land use of a sub-catchment of Freshwater Creek near Spalding, South Australia.* CSIRO, Adelaide.

MINTY B.R.S. 1997. Fundamentals of airborne gamma-ray spectrometry. *AGSO Journal of Australian Geology & Geophysics* **17**, 39 - 50.

MUNDAY T., WALKER G., CRESSWELL R., WILFORD J. R., BARNETT S. & COOK P. 2003. South Australian Salt Mapping and Management Support Project - An example of the considered application of airborne geophysics in natural resource management. *ASEG 16th Geophysical Conference and Exhibition*, Adelaide.

Rengasamy P. 2002. Transient salinity and subsoil constraints to dryland farming in Australian sodic soils: an overview. *Australian of Experimental Agriculture* **42,** 351 - 361.

Taylor G. & Eggleton R.A., 2001 *Regolith geology and geomorphology*. John Wiley and Sons, Ltd., Chichester, UK.